Available online at www.sciencedirect.com
SCIENCE DIRECT®
Biochimica et Biophysica Acta 1661 (2004) 135–143
BIOCHIMICA ET BIOPHYSICA ACTA
BBA
www.bba-direct.com

Membrane penetration of nitric oxide and its donor *S*-nitroso-*N*-acetylpenicillamine: a spin-label electron paramagnetic resonance spectroscopic study

Saviana Nedeianu[a], Tibor Páli[a,b,*], D. Marsh[b]

[a] *Institute of Biophysics, Biological Research Centre Szeged, P.O. Box 521, H-6701 Szeged, Hungary*
[b] *Abteilung Spektroskopie, Max-Planck-Institut für biophysikalische Chemie, 37070 Göttingen, Germany*

Received 1 October 2003; received in revised form 12 December 2003; accepted 15 December 2003

Abstract

S-nitroso-*N*-acetylpenicillamine (SNAP) is a pharmacological agent with diverse biological effects that are mainly attributable to its favorable characteristics as a nitric oxide (NO)-evolving agent. It is found that SNAP incorporates readily into dimyristoyl phosphatidylcholine (DMPC) bilayer membranes; and an approximate penetration profile was obtained from the depth dependence of the perturbation that it exerts on spin-labeled lipid chains. The profile of SNAP locates it deep in the hydrophobic core of both fluid- and gel-phase membranes. The spin relaxation enhancement of spin-labeled phospholipids with nitroxide group located at different depths in DMPC membranes was determined for nitric oxide (NO) and molecular oxygen (O_2), at close to atomic spatial resolution. The relaxation enhancement, which is proportional to the corresponding vertical membrane profile of the concentration-diffusion product, was measured in the gel and fluid phases of the lipid bilayer. No significant membrane penetration was observed in the gel phase for the two water-dissolved gases. In the fluid phase, the transmembrane profiles of NO and O_2 are similar and could be well described by a sigmoidal function with a maximum in the center of the bilayer, but that of NO is less steep and is shifted toward the center of the membrane, relative to that of O_2. These differences can be attributed mainly to the difference in hydrophobicity between the two gases and the presence of the donor in the NO experiments. The biological implications of the above results are discussed.

Keywords: Nitric oxide; NO donor; Membrane penetration; Electron paramagnetic resonance; Spin label; Spin relaxation enhancement

1. Introduction

The diverse biological functions of nitric oxide (NO) [1–6] keep it in the focus of biochemical research [7–10]. Nitric oxide, like oxygen, is a hydrophobic gas, hence biomembranes and other hydrophobic structures, such as low-density lipoproteins or hydrophobic regions of proteins, are potential sinks for NO and O_2. Because of the higher local concentrations and reduced possibility of hydrolysis reactions, NO, O_2, and their derived reactive species exhibit very different chemistry in these hydrophobic environments than in aqueous ones [11]. Indeed, many functions that are assigned to NO are membrane-associated [7], and at least one type of NO synthase contains a myristoylation site and is largely associated with (endothelial) cell membranes [12]. NO can inhibit cytochrome *c* oxidase rapidly and reversibly, which may be implicated in the cytotoxic effects of nitric oxide in the nervous system and other tissues [13]. In the heart, NO inhibits L-type Ca^{2+} channels but stimulates Ca^{2+} release from the sarcoplasmic reticulum, and the cardiac Ca-ATPase is also a membranous target of NO [9]. In human erythrocytes, hemoglobin-derived *S*-nitrosothiol, generated from imported NO, is associated predominantly with the red blood cell membrane [14].

Nitric oxide also plays a role in lipid biochemistry. While NO alone does not induce lipid peroxidation, it exhibits both stimulation and inhibition of superoxide- and peroxynitrite-dependent lipid peroxidation, depending on the ratio of the

Abbreviations: CW, continuous wave; DMPC, 1,2-dimyristoyl-*sn*-glycero-3-phosphocholine; EPR, electron paramagnetic resonance; NO, nitric oxide; *n*-PCSL, 1-acyl-2-[*n*-(4,4-dimethyloxazolidine-*N*-oxyl)stearoyl]-*sn*-glycero-3-phosphocholine; SNAP, *S*-nitroso-*N*-acetylpenicillamine

* Corresponding author. Institute of Biophysics, Biological Research Centre Szeged, P.O. Box 521, H-6701 Szeged, Hungary. Tel.: +36-62-599-603; fax: +36-62-433-133.
E-mail address: tpali@nucleus.szbk.u-szeged.hu (T. Páli).

0005-2736/$ - see front matter © 2004 Elsevier B.V. All rights reserved.
doi:10.1016/j.bbamem.2003.12.008

rate of production of reactive oxygen species to that of production of NO by donors such as *S*-nitroso-*N*-acetylpenicillamine (SNAP) and *S*-nitrosoglutathione [15]. It was found further that NO serves as a potent inhibitor of lipid peroxidation propagation reactions [16]. The high hydrophobicity of NO (it is about 10 times more soluble in hexane than in water [17]), its lipophilicity (see, e.g., Ref. [18]), its ability to diffuse rapidly in lipophilic environments [19], and its potent reactivity toward lipid radical species reveal its critical role in regulating membrane and lipoprotein lipid oxidation reactions [16].

Despite the above observations, the membrane penetration profiles of NO were largely neglected until relatively recently. Subczynski et al. [20] sampled the profile of the concentration-diffusion product of exogenously added NO, at four locations in the membrane, by using spin-labeled stearic acid analogs and electron paramagnetic resonance (EPR) line broadening measurements [20]. Quenching of pyrene fluorescence by NO and O_2 was used to probe their diffusion into/in the membrane by using fluorescent lipid derivatives located at two different vertical positions in the membrane [19]. Oxygen and nitric oxide were found to display similar diffusional behavior, and an increased solubility toward the center of the membrane.

Our aim here is to look at the penetration of NO into lipid membranes by using the potent NO donor SNAP, instead of exogenous NO gas. We wish to characterize the membrane penetration of the donor, because it is expected to release NO in membranes during in vivo applications. The choice of SNAP as the membrane-soluble NO donor was several fold: good thermal stability [21,22], release of NO at manageably slow rate [23], and both biological and therapeutic relevance (see later). The *S*-nitrosothiol class of NO donors, such as SNAP [24], has many biological activities that are related mainly to their NO storage, transfer, and delivery functions (see Ref. [25] for a recent review). Not only have they been suggested to generate intermediates in signal transduction, but also the decomposition of these compounds is of considerable biological relevance [26]. Immediately upon solubilization, SNAP evolves NO spontaneously by a single, irreversible, diffusion-controlled reduction step [27]. SNAP is one of the *S*-nitrosothiol NO donors used most for both in vivo and in vitro studies [25,28] and, like other *S*-nitrosothiols, has high therapeutic potential as an NO donor drug [23,29,30]. The solubility of SNAP is 2 mg/ml in water and 25 mg/ml in dimethylsulfoxide or ethanol (see, e.g., Bio-Stat catalogue (Stockport, GB) and Ref. [31]). Thus, it is expected that SNAP enters into lipid membranes [32,33], but little is known about its exact location in membrane bilayers.

In the present paper, we use spin-label EPR to study the localization of the SNAP NO donor in membranes of dimyristoyl phosphatidylcholine (DMPC), and to determine the vertical profile across the membrane of NO released from SNAP. This is done by investigating the effects of SNAP on the mobility of the spin-labeled lipid chains, and by measuring the enhancement of the spin-label relaxation by paramagnetic interaction with NO. To determine the transmembrane profiles at high vertical resolution, we use spin-labeled positional analogs of the host lipid that bear the nitroxide group at each position from C4 to C14 of the phosphatidylcholine *sn*-2 chain. The transmembrane profile for NO is compared with that for oxygen, which has been investigated in some detail recently [34]. Because there are numerous hydrophobic targets for NO, the present results are relevant not only to the use of SNAP-based *S*-nitrosothiols as NO donors, but also to the reactivity of NO in membranes and the consequent effects on cellular function.

2. Materials and methods

2.1. Materials

DMPC was obtained from Avanti Polar Lipids (Alabaster, AL). Spin-labeled phosphatidylcholines, *n*-PCSL (1-acyl-2-[*n*-(4,4-dimethyloxazolidine-*N*-oxyl)stearoyl]-*sn*-glycero-3-phosphocholine) with $n=4-14$ were synthesized according to Ref. [35]. The nitric oxide donor, SNAP, was purchased from Alexis Biochemicals (Lausen, Switzerland). Chloroform and methanol were from Merck (Darmstadt, Germany). Oxygen and argon gas (both of 99.9% purity) were purchased from Messer Griesheim GmbH (Frankfurt, Germany). Double-distilled water was used in all experiments and flushed with argon, except when indicated otherwise.

2.2. Sample preparation

DMPC stock solution (10 mg/ml) was prepared in a mixture of chloroform/methanol, 2:1 (v/v). Lipid spin labels (*n*-PCSL) were prepared as stock solutions in the same organic solvent mixture at a concentration of 1 mg/ml. The stock solutions were kept in the freezer before use. DMPC vesicles were labeled with *n*-PCSL at a mole ratio of either 4:100 or 1:800, as follows. The desired amount of *n*-PCSL ($n=4-14$) stock solution was added to 100 μl of the DMPC stock solution. After mixing, the solution was dried under nitrogen gas flow and then under vacuum overnight. The dry lipid film obtained was hydrated with 100 or 50 μl of water, in the high- and low-label concentration experiments, respectively, and loaded into a standard 1 mm (i.d.) EPR glass capillary. According to the particular experiment, argon or oxygen gas was flushed into the water, both before and after hydration of the lipid films. In some experiments, the samples were reflushed in the capillary with argon or oxygen and the EPR spectra were recorded again. In experiments with the NO donor, the dry lipid films were hydrated with water (flushed with either argon or oxygen) containing either 2 mM or a

saturating amount (~ 9 mM) of SNAP, for samples with label/lipid = 1:800 or 4:100 mol/mol, respectively. DMPC vesicles were pelleted in the EPR capillaries in a benchtop centrifuge at 10000 rpm for 10 min at room temperature. The supernatant and some lipid material was removed to leave a uniform pellet of 5 mm length, and the capillary was also filled with the requisite gas before being sealed for recording EPR spectra. Flushing of argon and oxygen into water was always done at 25 °C.

2.3. EPR spectroscopy and data analysis

EPR spectra were recorded on a Bruker (Rheinstetten, Germany) EMX X-band (9.3 GHz) spectrometer equipped with a TE_{102} cavity, using 100-kHz field modulation with a modulation amplitude of 1 G. Samples were positioned along the symmetry axis of the 4-mm standard quartz sample tube, which contained light silicone oil for thermal stability. The sample temperature was computer-controlled by a nitrogen gas-flow temperature system that regulated the temperature of the silicone oil. Samples were centered in the TE_{102} microwave cavity. Typically four spectra, of 1024 points each, were accumulated under critical coupling conditions over a 120-G scan range in 42-s scans, and digitally averaged to reduce noise. For continuous-wave power saturation experiments, a calibration was made between the microwave power output and the microwave field (H_1) incident on the sample, and corrections were also made for differences in cavity Q between different samples as described in Ref. [36]. Spectra were recorded at microwave powers ranging from 0.02 to 200 mW, at a temperature of either 10, 20, or 30 °C. All processing of EPR spectra, including determination of peak-to-peak distances, as well as fitting, processing, and presentation of the data and CW saturation curves, was performed using Igor (WaveMetrics, Lake Oswego, OR) with software written by one of us (T.P.). Integration of the spectra was done either with Igor or with WinEPR (Bruker, Karlsruhe).

3. Results and discussion

3.1. Lipid chain perturbation by SNAP

EPR spectra of positional isomers, *n*-PCSL, of spin-labeled PC in DMPC membranes, at 10 and 30 °C, in the absence and presence of SNAP, are shown in Fig. 1. In these experiments, a label/lipid molar ratio of 4:100 was used. This relatively high value served to detect effects of SNAP on spin–spin interactions between the spin labels. Samples were deoxygenated and SNAP was administered at a saturating aqueous concentration (~ 9 mM). The control spectra show relatively broad lines in the gel phase (10 °C, Fig. 1A), which is due partly to spin–spin interaction between the spin labels. This effect, which dominates the line shape at spin-label positions $n = 8–12$, is due to partial segregation of the *n*-PCSL molecules in gel-phase DMPC, as observed earlier with dipalmitoyl phosphatidylcholine [37]. The presence of SNAP reduces this spin–spin interaction very significantly. In fluid-phase DMPC (30 °C; Fig. 1B), where spin label segregation is absent, SNAP exerts a strong perturbing effect on the spectra that increases progressively toward positions C10–C11.

The effect of SNAP on lipid chain dynamics was quantitated by measuring the outer hyperfine splitting of the *n*-PCSL spin labels, in the absence and presence of the NO donor. Fig. 2 shows the difference, at 10 and 30 °C, in the outer splitting as a function of the position, *n*, of the doxyl group in the acyl chain of the spin-labeled PC. In the gel phase, SNAP has largest effect in the middle of the bilayer and this effect shows a monotonic dependence on *n*. (It should be noted that, for $n = 10–12$, a small contribution to the changes observed in the outer splitting originates from weakening the spin–spin interaction between labels by SNAP.) In the fluid phase (30 °C), the positional dependence of the chain perturbation is qualitatively similar (but has the opposite sign), and the largest effect is detected for positions $n = 10–14$.

The effect of SNAP on the spin-label segregation in the gel phase is more evident in Fig. 3, in which spin relaxation parameters are presented because these are more sensitive to spin–spin interactions. Progressive (CW) saturation data were analyzed by fitting the dependence of the spectral second integral, *I*, on microwave field (H_1) with the following saturation curve [38]:

$$I = \frac{(\mathrm{d}I/\mathrm{d}H_1)_o H_1}{\sqrt{1 + \gamma_e^2 T_1 T_2 H_1^2}} \quad (1)$$

where $(\mathrm{d}I/\mathrm{d}H_1)_o$ is the linear slope at low power, γ_e is the electron gyromagnetic ratio, and T_1T_2 is the effective spin relaxation time product. The latter is sensitive to spin–spin interactions (see, e.g., Ref. [39]). Fig. 3 shows the effective relaxation rate product $1/(T_1T_2)$ of PC spin labels in DMPC membranes at 10 °C in the presence of SNAP for samples preflushed with argon, relative to samples prepared in the absence of SNAP and flushed with argon, as a function of the spin-label position, *n*. The relaxation "enhancement" is negative for all values of *n*. Because NO is known to enhance—rather than to deenhance—spin relaxation of spin labels in membranes [40], this confirms that the spectral effects observed in the gel phase of DMPC at ~ 9 mM aqueous SNAP are due to the donor alone and not to the released NO. The reduction in rate of spin relaxation can be explained by the dilution of the segregated spin label patches by SNAP incorporated in the membrane. Consequently, this negative enhancement does not follow the perturbation profile of lipid chain mobility by SNAP (Fig. 2); it is largest where the spin-label segregation is most pronounced, i.e., at $n = 8–12$, in agreement with Fig. 1A and earlier observations [37]. The above results demonstrate that SNAP incorporates massively in DMPC and certainly other

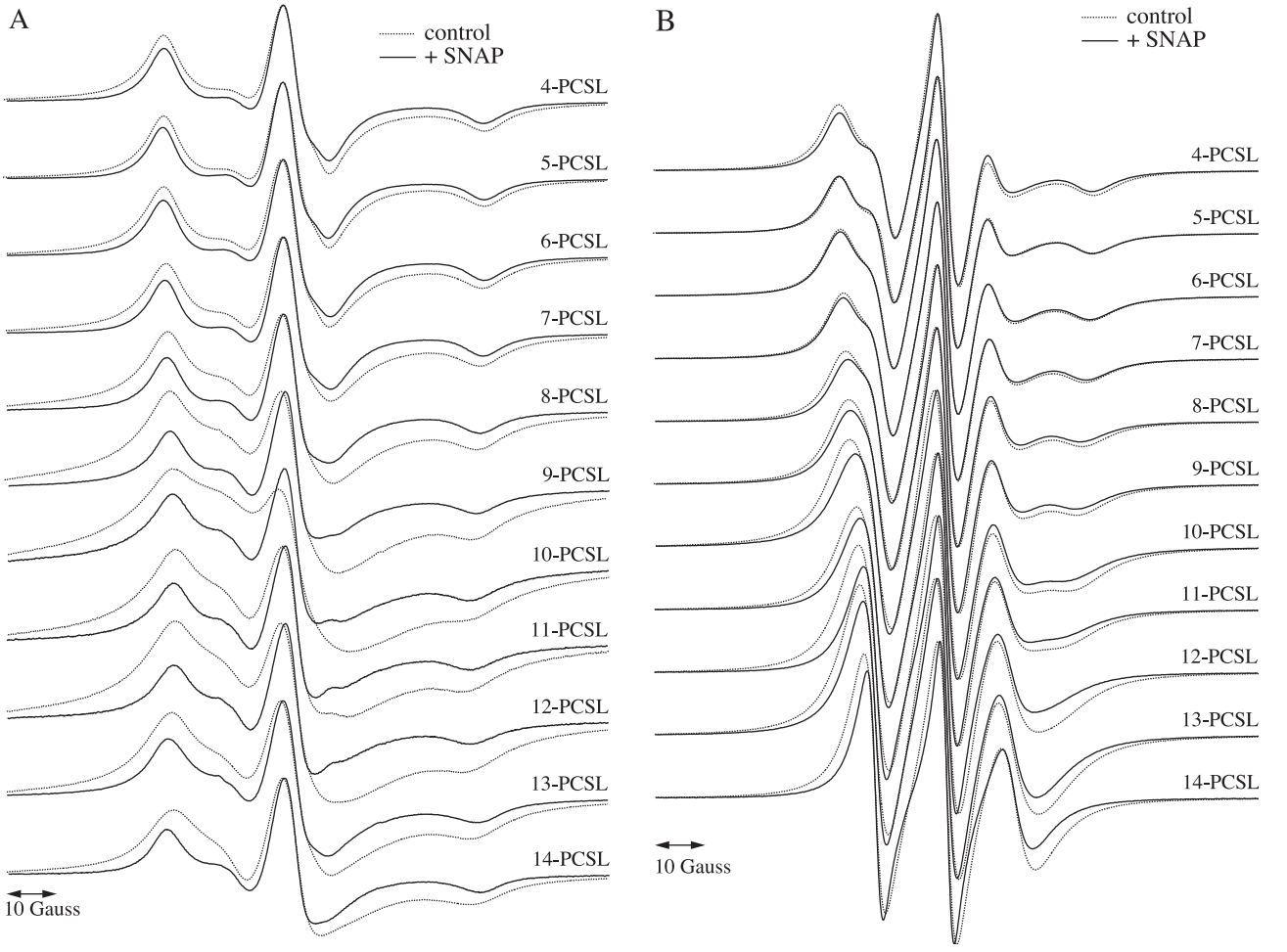

Fig. 1. EPR spectra of PC spin-label positional isomers, *n*-PCSL (as indicated for each spectrum pair) in DMPC membranes at 10 °C (panel A) and at 30 °C (panel B) in the absence (dotted lines) and presence (solid lines) of saturating aqueous concentration (~ 9 mM) of the nitric oxide donor SNAP. Spectra were recorded at a microwave power of 5 mW and are scaled to the same maximum amplitude. The spin label/lipid molar ratio is 4:100.

membranes, where it is situated in the hydrophobic core of the bilayer.

3.2. Penetration of nitric oxide and oxygen into phospholipid bilayers

The penetration profiles of NO and O_2 into DMPC membranes were monitored by the relaxation enhancement of the *n*-PCSL spin labels that is induced by these paramagnetic relaxants. The spin label/lipid molar ratio was 1:800, and the aqueous concentration of SNAP was 2 mM. Typical CW progressive saturation curves for 4-PCSL at 10 and 30 °C, and for 14-PCSL at 10 °C, are shown in Fig. 4. The dependence of the integrated intensities on the microwave field strength (H_1) are normalized to the same initial slope $(dI/dH_1)_0$ and are fitted according to Eq. (1). Curves that saturate less readily (e.g., 14-PCSL at 10 °C or 4-PCSL at 30 °C) indicate faster relaxation rate products (i.e., larger $1/T_1T_2$). The effective spin relaxation time product (T_1T_2), obtained from such CW progressive saturation experiments, is presented in Fig. 5 as a function of the spin-label position, *n*, of the PC spin label in DMPC membranes, at the different temperatures indicated. Both the hydrating media and the samples were flushed extensively with argon. The value of T_1T_2 is determined primarily by the dynamics of the spin-label group, i.e., by the rate, amplitude, and symmetry of its rotational diffusion. Because these dynamic features increase in intensity toward the center of the bilayer [41,42], the T_1T_2 product decreases monotonically. It also decreases with increasing temperature. These intrinsic values serve as reference for SNAP- and O_2-treated samples. Any type of spin–spin interaction decreases the value of T_1T_2 (i.e., a relaxation enhancement). At a label/lipid molar ratio of 1:800, spin–spin interaction between spin labels has negligible effect on T_1T_2 (see, e.g., Ref. [43]).

Fig. 6 gives the relaxation enhancement parameter, $R = \Delta(1/\Delta H_{pp}T_1T_2)$, for NO and O_2, relative to corresponding argon-flushed samples, as a function of the spin-label position *n* of the *n*-PCSL probes, in both gel- and fluid-phase DMPC membranes. Oxygen was introduced into the

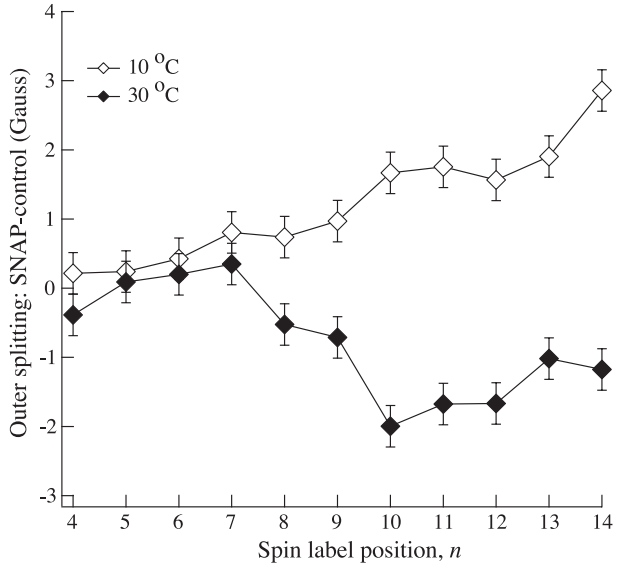

Fig. 2. Changes in the outer hyperfine splitting of spin-labeled PC, bearing the doxyl group at different positions along the *sn*-2 acyl chain (given in the *x* axis), induced by the presence of saturating aqueous concentration (~ 9 mM) of the nitric oxide donor SNAP. The label/lipid ratio is 4:100, the temperature is 10 and 30 °C for gel- and fluid-phase membranes, respectively.

samples by flushing the buffers and hydrated lipid samples, and filling the sample capillaries before sealing them. Control samples were flushed similarly but with argon. Nitric oxide was released by SNAP in samples flushed with argon. The samples were always freshly prepared and measured as quickly as possible. Because the diffusion of NO is fast compared with its release by SNAP [28], with the

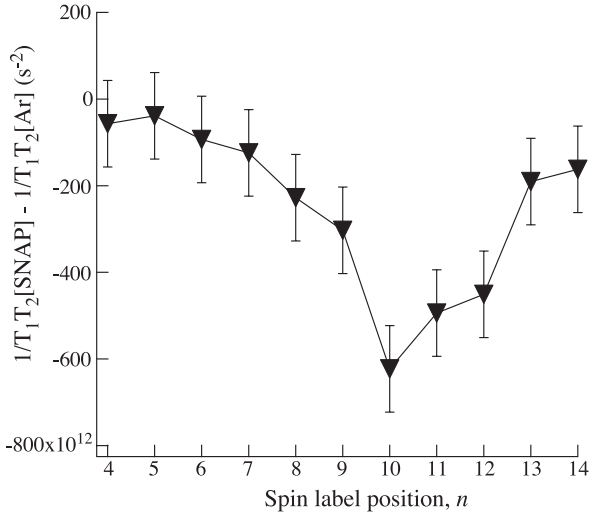

Fig. 3. Changes in the effective relaxation rate product $1/T_1T_2$ of PC spin labels in DMPC membranes at 10 °C shown as a function of the position, *n*, of the doxyl group along the hydrocarbon chain of the spin-labeled lipid molecule. The changes show the effect of the presence of the NO donor SNAP (~ 9 mM) in samples preflushed with argon relative to samples made in the absence of SNAP and flushed with argon. Other experimental conditions are identical with those of Fig. 1.

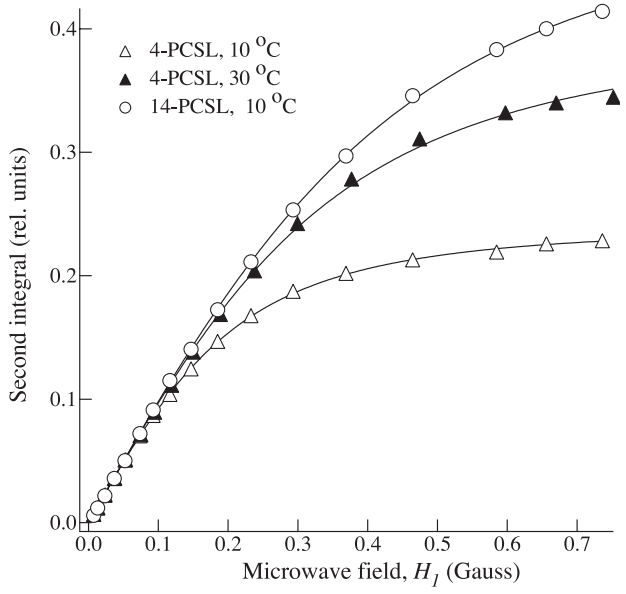

Fig. 4. CW saturation curves for double-integrated spectral intensity, as a function of the microwave field (H_1) incident on samples of PCSL spin labels (4- and 14-PCSL) incorporated into DMPC vesicles at a label/lipid molar ratio of 1:800, measured at the temperatures indicated. The second integrals are scaled to the same starting slope to aid comparison. The experimental values (symbols) were least-squares fitted according to Eq. (1) (solid lines).

size of the membrane [44], and with the time scale of our experiment, the transmembrane profile is proportional to the local steady state concentration-diffusion product of NO [45]. The rate of NO release from SNAP in this system,

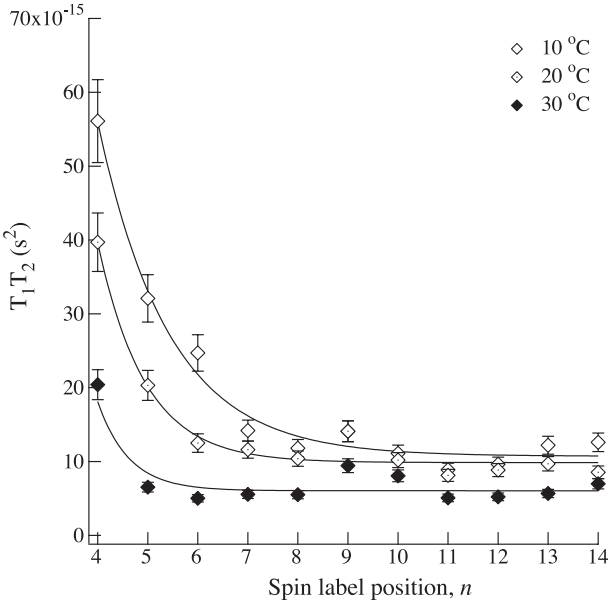

Fig. 5. Effective spin relaxation time product (T_1T_2) as a function of the position of the doxyl group along the *sn*-2 chain of spin-labeled PC molecules (*n*-PCSL) in DMPC membrane vesicles, at a molar ratio of label/lipid = 1:800 and the temperatures indicated. Both the hydrating media and the samples were flushed extensively with argon. The solid lines are fitted with single exponentials for the sole purpose of comparison.

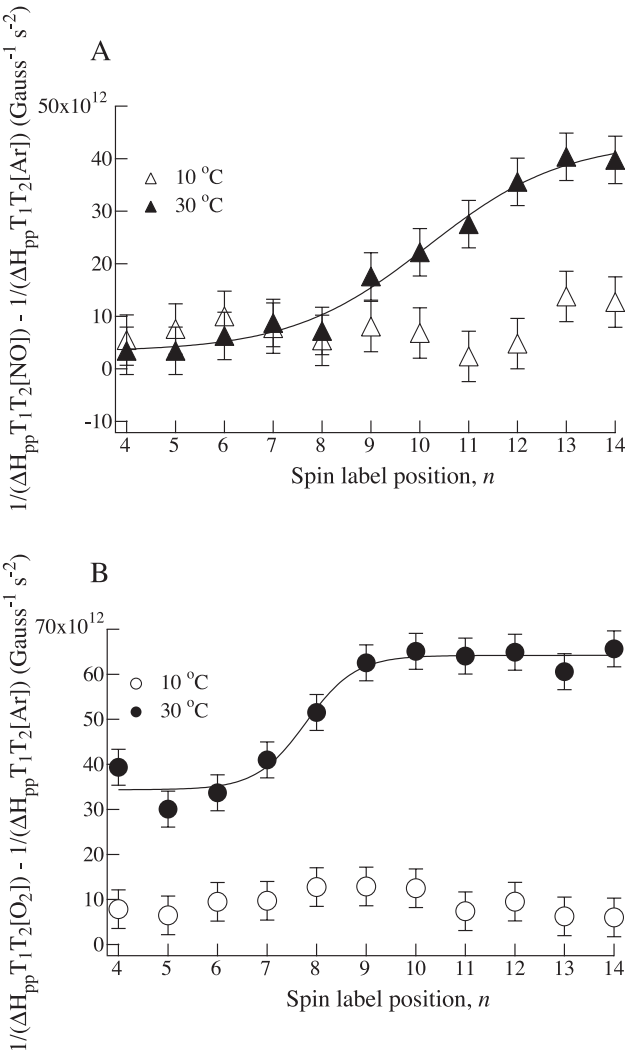

Fig. 6. Spin relaxation enhancement, $R = \Delta(1/\Delta H_{pp}T_1T_2)$, by nitric oxide (panel A), and by oxygen (panel B), of the positional spin label isomers (n-PCSL) in DMPC membranes in the gel (10 °C) and fluid (30 °C) phases. The label/lipid molar ratio was 1:800. The solid lines are least-squares fits of Eq. (3) with parameters $n_o = 10.2 \pm 0.3$, $\lambda = 1.4 \pm 0.3$ and $n_o = 7.8 \pm 0.2$, $\lambda = 0.5 \pm 0.2$ for the nitric oxide and oxygen data, respectively.

which nevertheless lacks metal ions, light, and reducing agents known to influence the release rate, is not known but the shape of the CW saturation curves (Fig. 4) and the relaxation profiles (Figs. 5 and 6) exclude the possibility of large variations in the membranous NO concentration. This is in agreement with the observation of an EPR signal of spin-trapped NO released by SNAP under anaerobic conditions, which was stable for several days (unpublished).

The fact that we see no relaxation enhancement in the rigid gel phase supports the earlier observation that the spin–spin interaction between the spin labels and the paramagnetic gases NO and O_2 is exclusively of the Heisenberg spin-exchange type [34,40], in which the relaxant comes into direct contact with the spin label, so that the spin orbitals overlap. The enhancement in spin-lattice relaxation rate, $1/T_1$, is proportional to the local concentration-diffusion product of the relaxant [46,47]:

$$\frac{1}{T_1} = \frac{1}{T_{1,0}} + k_0 D_R(z) c_R(z) \tag{2}$$

where $T_{1,0}$ is the spin-lattice relaxation time in the absence of relaxant, k_0 is a constant that depends on the structure of the interacting molecules, and $D_R(z)$ and $c_R(z)$ are the diffusion constant and local concentration of the relaxant, respectively, at vertical position z along the membrane normal. A similar equation applies to T_2, but because T_2 is about 2 orders of magnitude smaller than T_1 for nitroxide spin labels, the relative enhancement in $1/T_2$ is negligible compared with that in $1/T_1$ [39]. The relaxation enhancement parameter $1/T_1T_2$ was therefore corrected with the peak-to-peak width ΔH_{pp} of the central line, to reduce differences between different spin labels and to minimize the potential effect of SNAP on the line shape [48].

The permeation of small electrolytes (metal ions) but also nonelectrolytes (O_2 and possibly NO) into the membrane is strongly dependent on the polarity profile of the membrane [49]. It is therefore not surprising that the permeability profiles of NO and O_2 that are shown in Fig. 6 are similar, but are in the opposite sense, of course, to the polarity profile of DMPC bilayers [49]. The trough-like dependences of the relaxation enhancement, R, of NO and O_2 observed at low concentration of n-PCSL (with $n = 4–14$) spin labels in fluid DMPC membranes were fitted with a sigmoidal function according to Ref. [49]:

$$\Delta\left(\frac{1}{\Delta H_{pp} T_1 T_2}\right) = \frac{R_1 - R_2}{1 + \exp[(n - n_0)/\lambda]} + R_2 \tag{3}$$

where R_1 and R_2 are the base and maximum values of the sigmoid, n_o is the point of maximum gradient, and λ is the decay constant. The fitting parameters obtained for the 30 °C data are $R_1 = (3.3 \pm 1.6) \times 10^{12}\ G^{-1}\ s^{-2}$, $R_2 - R_1 = (4.0 \pm 0.4) \times 10^{13}\ G^{-1}\ s^{-2}$, $n_o = 10.2 \pm 0.3$ and $\lambda = 1.4 \pm 0.3$ for NO; and $R_1 = (3.4 \pm 0.2) \times 10^{13}\ G^{-1}\ s^{-2}$, $R_2 - R_1 = (3.0 \pm 0.3) \times 10^{13}\ G^{-1}\ s^{-2}$, $n_o = 7.8 \pm 0.2$ and $\lambda = 0.5 \pm 0.2$ for O_2. These enhancements were abolished when the samples were reflushed with argon (data not shown). Although the extents, $(R_2 - R_1)$, of the NO and O_2 fluid-phase profiles are comparable, the profile of NO permeability appears to be shifted down relative to that of O_2 by about $3.1 \times 10^{13}\ G^{-1}\ s^{-2}$. This difference may be attributed to (i) the presence of argon in the NO samples, which was needed to remove oxygen; (ii) the possibly lower concentration of NO than O_2 in the membrane (in their respective samples); and (iii) the presence of the donor in the NO samples (cf. Fig. 2). Some of the differences also may be attributed to the difference in the polarity of NO and O_2. While O_2 is nonpolar with zero dipole moment, that for NO is 0.159 Debye [50], which also may be responsible for the less steep profile and lower partitioning of NO compared to O_2.

Spin relaxation enhancement by molecular oxygen of spin labels in membranes, via Heisenberg spin exchange, was introduced for oximetry by Strzalka et al. [51] and has been studied extensively by Hyde et al. [45,52,53]. The same authors have also measured the permeability of nitric oxide through lipid bilayer membranes [20]. Our profile of relaxation enhancement is qualitatively similar to that of Ref. [20], but is spatially better resolved. In the work by Hyde et al. [45,52], the profile of NO was similar to that of O_2, in agreement with more limited fluorescence quenching data [19]. In addition, cholesterol increased the maximum in the profile of NO permeability and shifted it deeper into the hydrophobic core of the membrane [20]. SNAP itself is quite hydrophobic and has a molecular mass of 220 Da, which is smaller than that of cholesterol (387 Da) but SNAP dimerizes via S–S bridges after releasing NO [25]. Therefore, a perturbing effect of SNAP on the NO profile can be anticipated. It is clear from Fig. 2 that SNAP perturbs the mobility of the lipid chains, although in a different way from that of cholesterol. At least part of the shift and broadening of the NO profile, relative to that for O_2, may therefore be attributed to the incorporation of the NO donor into the hydrophobic interior of the membrane. In particular, because perturbation by the donor reaches a plateau at positions $n=10-11$ in the fluid membrane, it is very likely to influence and possibly broaden the profile of NO relative to that of O_2 for which no donor was used.

3.3. Membrane concentrations and permeability to nitric oxide

The relaxation-rate enhancements, $R=\Delta(1/\Delta H_{pp}T_1T_2)$, for the nitroxides at position n that are given in Fig. 6, are directly proportional to the product $K_R(n)D_R(n)$ of the local partition and diffusion coefficients of the relaxant in the membrane (see Eq. (2)). Because of their comparable molecular size, the diffusion coefficients of NO and oxygen are likely to be similar. (In water at 20 °C, $D_w=2.35$ and 2.00×10^{-5} cm^2 s^{-1} for NO and O_2, respectively [50].) Comparison of the results in Figs. 6A,B therefore shows that the steady state concentration of NO produced by SNAP in the center of the membrane is approximately two thirds of the equilibrium concentration of oxygen. For oxygen, it was found that the partition-diffusion product at the interfacial region of the membrane is $K_1D_1\approx5\times10^{-5}$ cm^2 s^{-1} [34]. From Fig. 6B, the partition-diffusion product of oxygen at the center of the membrane then becomes $K_2D_2=K_1D_1\times(R_2/R_1)\approx10^{-4}$ cm^2 s^{-1} (cf. Eq. (3)). Therefore, the partition-diffusion product for nitric oxide in the center of the membrane is: $K_2D_2\approx7\times10^{-5}$ cm^2 s^{-1}, under steady state NO evolution by SNAP. This is the quantity that determines the rate of reactions with NO within the membrane. Comparison with the diffusion coefficient of NO in water ($D_w=2.35\times10^{-5}$ cm^2 s^{-1} at 20 °C), shows that NO reaction rates in the membrane are potentially three times higher than those in the aqueous phase.

The transmembrane profile given in Fig. 6A can be used to determine the membrane permeability to nitric oxide. Previous estimates have used far fewer points to define the profile [20]. The contribution to the permeability barrier, $1/P$, is given by:

$$\delta(1/P)\int_0^{2d}\frac{dz}{K(z)D(z)} \tag{4}$$

where $K(z)$ and $D(z)$ are the local partition and diffusion coefficients, respectively, for NO at distance z into the membrane of total thickness, $2d$. Using the transmembrane profile given by Eq. (3), together with Eq. (4), results in [49]:

$$\delta(1/P)=\frac{2}{K_1D_1}\left[d+\lambda\left(\frac{K_1D_1}{K_2D_2}-1\right)\times ln\left(\frac{K_1D_1/K_2D_2+e^{(d-d_o)/\lambda}}{k_1D_1/K_2D_2+e^{-d_o/\lambda}}\right)\right] \tag{5}$$

where d_o is the distance corresponding to chain position n_o, and λ is also expressed as a distance. For fluid DMPC bilayers, the width of the membrane is $2d\approx3$ nm with an increment of 0.1 nm per methylene group [54]. Using the relaxation enhancement data from above, it is found that the hydrophobic membrane core actually enhances the NO permeability, which is increased by a factor of $2\times$, relative to that in a uniform membrane with fixed partition and diffusion coefficients, K_1 and D_1. Thus, membranes can form effective channels of communication for efficient NO transport within cells. Taking $K_1D_1\approx D_w$ from the spin-label linebroadening results of Subczynski et al. [20], with $D_w=2.35\times10^{-5}$ cm^2 s^{-1} for the diffusion coefficient of NO in water [50], yields an effective permeability coefficient $P=160$ cm s^{-1} for NO in fluid DMPC bilayers.

4. Conclusions

Direct or indirect membranous targets of NO, such as C=C unsaturated bonds or certain amino acid side chains, have defined vertical location in biological membranes. Therefore, the membrane penetration profiles of NO, of its derived reactive species, and of its potent hydrophobic donors, are of considerable biological and biochemical relevance. Being diffusion-controlled, most of the chemical reactions of NO depend on the rate of collision of NO with the target molecules or functional groups. The collision rate between NO and its target is proportional to the concentration-diffusion product of NO, which is determined at high vertical resolution for a phospholipid bilayer in the present study. This allowed us to observe differences between NO and O_2 and also to locate SNAP in the membrane. In addition, this is the first systematic study to look at the effect of this important NO donor on a phospholipid membrane.

Because the profiles of NO and O_2 are qualitatively similar, chemical reactions in the membrane involving NO or O_2 will proceed at higher rates in the center of the bilayer than in the phospholipid headgroup region. For instance, whereas NO is protected from hydrolysis-related reactions in the center of the membrane, products of NO autooxidation are likely to be present in membranes whenever free O_2 is available. As an example, the rate of NO autooxidation is orders of magnitudes higher, if a hydrophobic lipid phase (soy phospholipid vesicles, nonionic detergents, or membranes isolated from rat hepatocytes) is present, than in an otherwise entirely hydrophilic environment [55]. The fact that tissues producing NO, such as liver or brain, contain a relatively high concentration of phospholipids, combined with the NO profile presented here, suggests that most of the NO-dependent reactions take place in the hydrophobic core of biomembranes. These reactions display a strong depth dependence (see Fig. 6), which is amplified if O_2-dependent NO reactions are considered. Combined with this, the fact that SNAP also concentrates in the hydrophobic core of the bilayer is one of the reasons why it is an effective and functional NO donor in in vivo experiments.

Membrane proteins that are structurally or functionally dependent on amine, thiol, tyrosine (radical), or heme groups, or on ternary iron complexes, are all likely to be direct, or indirect, targets of NO [7]. The rate of reaction between NO and such targets that are located in the transmembrane secondary structure of integral proteins will be proportional to the local concentration-diffusion product. Hence, the reaction rate will show a strong dependence on the vertical membrane location of the target residue, in addition to depending on the extent to which the target is exposed to the lipid phase or embedded within the protein. This is similar to the case of oxygen, the relaxation enhancement by which has been used extensively to locate the position of spin-labeled residues of membrane proteins in the bilayer [48,56–58]. Likewise, lipid peroxidation reactions should also show a strong dependence on the vertical location of the double bonds along the acyl chain. The present results suggest that the hydrophobic core of a fluid membrane is one primary site of NO-dependent chemistry in biological systems that should have a strong dependence on the vertical position in the membrane. Finally, the large difference observed between the gel- and fluid-membrane phases suggests that NO and O_2 should display significant heterogeneity in their lateral membrane distribution, if the host biomembrane contains domains (patches, rafts, etc.) of different composition or different lipid chain dynamics.

Acknowledgements

We thank Frau B. Angerstein for the synthesis of spin-labeled phospholipids. This work was supported by German–Hungarian travel grants (DAAD-324/PPP, MÖB-D18/2001 and BMBF-00/16, TéT-D27/00) and in part by the Hungarian Ministry of Health (T08003/99) and the Hungarian National Research Fund (OTKA T043425). S.N. was a recipient of a short-term FEBS fellowship.

References

[1] D.E. Koshland, The molecule of the year, Science 258 (1992) 1861.
[2] M. Delledonne, Y.J. Xia, R.A. Dixon, C. Lamb, Nitric oxide functions as a signal in plant disease resistance, Nature 394 (1998) 585–588.
[3] L.J. Ignarro, Nitric oxide: a unique endogenous signaling molecule in vascular biology (Nobel lecture), Angew. Chem., Int. Ed. 38 (1999) 1882–1892.
[4] F. Murad, Discovery of some of the biological effects of nitric oxide and its role in cell signaling, Biosci. Rep. 19 (1999) 133–154.
[5] F. Murad, The excitement and rewards of research with our discovery of some of the biological effects of nitric oxide, Circ. Res. 92 (2003) 339–341.
[6] K. Bian, F. Murad, Nitric oxide (NO) - biogeneration, regulation, and relevance to human diseases, Front. Biosci. 8 (2003) D264–D278.
[7] D.A. Wink, J.B. Mitchell, Chemical biology of nitric oxide: insights into regulatory, cytotoxic, and cytoprotective mechanisms of nitric oxide, Free Radic. Biol. Med. 25 (1998) 434–456.
[8] K.L. Davis, E. Martin, I.V. Turko, F. Murad, Novel effects of nitric oxide, Annu. Rev. Pharmacol. Toxicol. 41 (2001) 203–236.
[9] L.A. Barouch, R.W. Harrison, M.W. Skaf, G.O. Rosas, T.P. Cappola, Z.A. Kobeissi, I.A. Hobai, C.A. Lemmon, A.L. Burnett, B. O'Rourke, E.R. Rodriguez, P.L. Huang, J.A.C. Lima, D.E. Berkowitz, J.M. Hare, Nitric oxide regulates the heart by spatial confinement of nitric oxide synthase isoforms, Nature 416 (2002) 337–340.
[10] E. Nisoli, E. Clementi, C. Paolucci, V. Cozzi, C. Tonello, C. Sciorati, R. Bracale, A. Valerio, M. Francolini, S. Moncada, M.O. Carruba, Mitochondrial biogenesis in mammals: the role of endogenous nitric oxide, Science (2003) 899.
[11] S.P.A. Goss, R.J. Singh, N. Hogg, B. Kalyanaraman, Reactions of .NO, $.NO_2$ and peroxinitrite in membranes: physiological implications, Free Radic. Res. 31 (1990) 597–606.
[12] O.W. Griffith, D.J. Stuehr, Nitric oxide synthases: properties and catalytic mechanism, Annu. Rev. Physiol. 57 (1995) 707–736.
[13] M.W.J. Cleeter, J.M. Cooper, V.M. Darley-Usmar, S. Moncada, A.H.V. Schapira, Reversible inhibition of cytochrome *c* oxidase, the terminal enzyme of the mitochondrial respiratory chain, by nitric oxide—implications for neurodegenerative diseases, FEBS Lett. 345 (1994) 50–54.
[14] J.R. Pawloski, D.T. Hess, J.S. Stamler, Export by red blood cells of nitric oxide bioactivity, Nature 409 (2001) 622–626.
[15] H. Rubbo, R. Radi, M. Trujillo, R. Telleri, B. Kalyanaraman, S. Barnes, M. Kirk, B.A. Freeman, Nitric oxide regulation of superoxide and peroxynitrite-dependent lipid peroxidation—formation of novel nitrogen-containing oxidized lipid derivatives, J. Biol. Chem. 269 (1994) 26066–26075.
[16] H. Rubbo, R. Radi, D. Anselmi, M. Kirk, S. Barnes, J. Butler, J.P. Eiserich, B.A. Freeman, Nitric oxide reaction with lipid peroxyl radicals spares α-tocopherol during lipid peroxidation—greater oxidant protection from the pair nitric oxide/α-tocopherol than α-tocopherol/ascorbate, J. Biol. Chem. 275 (2000) 10812–10818.
[17] M.H. Abraham, J.M.R. Gola, J.E. Cometto-Muniz, W.S. Cain, The solvation properties of nitric oxide, J. Chem. Soc., Perkin Trans. 2 (2000) 2067–2070.
[18] N. Marchettini, M. Rustici, M. Branca, N. Culeddu, M. Fruianu, M.V. Serra, E. Tiezzi, Solubility of nitric oxide (NO) in lipid aggregates as monitored by nuclear magnetic resonance, Colloids Surf. 131 (1998) 1–6.
[19] A. Denicola, J.M. Souza, R. Radi, E. Lissi, Nitric oxide diffusion in

membranes determined by fluorescence quenching, Arch. Biochem. Biophys. 328 (1996) 208–212.
[20] W.K. Subczynski, M. Lomnicka, J.S. Hyde, Permeability of nitric oxide through lipid bilayer membranes, Free Radic. Res. Commun. 24 (1996) 343–349.
[21] N. Bainbrigge, A.R. Butler, C.H. Gorbitz, The thermal stability of *S*-nitrosothiols: experimental studies and ab initio calculations on model compounds, J. Chem. Soc., Perkin Trans. 2 (1997) 351–353.
[22] K. Goto, Y. Hino, T. Kawashima, M. Kaminaga, E. Yano, G. Yamamoto, N. Takagi, S. Nagase, Synthesis and crystal structure of a stable *S*-nitrosothiol bearing a novel steric protection group and of the corresponding *S*-nitrothiol, Tetrahedron Lett. 41 (2000) 8479–8483.
[23] I.L. Megson, I.R. Greig, A.R. Butler, G.A. Gray, D.J. Webb, Therapeutic potential of *S*-nitrosothiols as nitric oxide donor drugs, Scott. Med. J. 42 (1997) 88–89.
[24] C. Napoli, L.J. Ignarro, Nitric oxide-releasing drugs, Annu. Rev. Pharmacol. Toxicol. 43 (2003) 97–123.
[25] P.G. Wang, H. Xie, X.P. Tang, X.J. Wu, Z. Wen, T.W. Cai, A.J. Janczuk, Nitric oxide donors: chemical activities and biological applications, Chem. Rev. 102 (2002) 1091–1134.
[26] R.J. Singh, N. Hogg, J. Joseph, B. Kalyanaraman, Mechanism of nitric oxide release from *S*-nitrosothiols, J. Biol. Chem. 271 (1996) 18596–18603.
[27] Y.C. Hou, J.Q. Wang, F. Arias, L. Echegoyen, P.G. Wang, Electrochemical studies of *S*-nitrosothiols, Bioorg. Med. Chem. Lett. 8 (1998) 3065–3070.
[28] I.L. Megson, I.R. Greig, G.A. Gray, D.J. Webb, A.R. Butler, Prolonged effect of a novel *S*-nitrosated glyco amino acid in endothelium-denuded rat femoral arteries: potential as a slow release nitric oxide donor drug, Br. J. Pharmacol. 122 (1997) 1617–1624.
[29] H.H. Gutierrez, B. Nieves, P. Chumley, A. Rivera, B.A. Freeman, Nitric oxide regulation of superoxide-dependent lung injury: oxidant-protective actions of endogenously produced and exogenously administered nitric oxide, Free Radic. Biol. Med. 21 (1996) 43–52.
[30] N. Hogg, B. Kalyanaraman, J. Joseph, A. Struck, S. Parthasarathy, Inhibition of low density lipoprotein oxidation by nitric oxide—potential role in atherogenesis, FEBS Lett. 334 (1993) 170–174.
[31] J. Ramirez, L.B. Yu, J. Li, P.G. Braunschweiger, P.G. Wang, Glyco-*S*-nitrosothiols, a novel class of NO donor compounds, Bioorg. Med. Chem. Lett. 6 (1996) 2575–2580.
[32] G.E. Carnahan, P.G. Lenhert, R. Ravichandran, *S*-nitroso-*n*-acetyl-DL-penicillamine, Acta Crystallogr., B 34 (1978) 2645–2648.
[33] L.R. Field, R.V. Dilts, R. Ravichandran, P.G. Lenhert, G.E. Carnahan, Unusually stable thionitrite from *n*-acetyl-D,L-penicillamine—X-ray crystal and molecular structure of 2-(acetylamino)-2-carboxy-1,1-dimethylethyl thionitrite, J. Chem. Soc., Chem. Commun. 6 (1978) 249–250.
[34] B.G. Dzikovski, V.A. Livshits, D. Marsh, Oxygen permeation profile in lipid membranes: non-linear spin-label EPR, Biophys. J. 85 (2003) 1005–1012.
[35] D. Marsh, A. Watts, Spin-labeling and lipid–protein interactions in membranes, in: P.C. Jost, O.H. Griffith (Eds.), Lipid–Protein Interactions, vol. 2, Wiley-Interscience, New York, 1982, pp. 53–126.
[36] P. Fajer, D. Marsh, Microwave and modulation field inhomogeneities and the effect of cavity Q in saturation transfer ESR spectra. Dependence on sample size, J. Magn. Reson. 49 (1982) 212–224.
[37] P. Fajer, A. Watts, D. Marsh, Saturation transfer, continuous wave saturation, and saturation recovery electron spin resonance studies of chain-spin labeled phosphatidylcholines in the low temperature phases of dipalmitoyl phosphatidylcholine bilayers. Effects of rotational dynamics and spin–spin interactions, Biophys. J. 61 (1992) 879–891.
[38] T. Páli, L.I. Horváth, D. Marsh, Continuous-wave saturation of two-component, inhomogeneously broadened, anisotropic EPR spectra, J. Magn. Reson., A 101 (1993) 215–219.
[39] V.A. Livshits, T. Páli, D. Marsh, Relaxation time determinations by progressive saturation EPR: effects of molecular motion and Zeeman modulation for spin labels, J. Magn. Reson. 133 (1998) 79–91.
[40] R.J. Singh, N. Hogg, H.S. Mchaourab, B. Kalyanaraman, Physical and chemical interactions between nitric oxide and nitroxides, Biochim. Biophys. Acta 1201 (1994) 437–441.
[41] H.M. McConnell, Molecular motion in biological membranes, in: L.J. Berliner (Ed.), Spin Labeling. Theory and Applications, vol. 1, Academic Press, New York, 1976, pp. 525–560.
[42] M. Moser, D. Marsh, P. Meier, K.-H. Wassmer, G. Kothe, Chain configuration and flexibility gradient in phospholipid membranes. Comparison between spin-label electron spin resonance and deuteron nuclear magnetic resonance, and identification of new conformations, Biophys. J. 55 (1989) 111–123.
[43] T. Páli, V.A. Livshits, D. Marsh, Dependence of saturation-transfer EPR intensities on spin-lattice relaxation, J. Magn. Reson., B 113 (1996) 151–159.
[44] J.R. Lancaster, Simulation of the diffusion and reaction of endogenously produced nitric oxide, Proc. Natl. Acad. Sci. U. S. A. 91 (1994) 8137–8141.
[45] W.K. Subczynski, J.S. Hyde, A. Kusumi, Oxygen permeability of phosphatidylcholine–cholesterol membranes, Proc. Natl. Acad. Sci. U. S. A. 86 (1989) 4474–4478.
[46] W. Subczynski, J.S. Hyde, The diffusion concentration product of oxygen in lipid bilayers using the spin-label T_1 method, Biochim. Biophys. Acta 643 (1981) 283–291.
[47] V.A. Livshits, B.G. Dzikovski, D. Marsh, Mechanism of relaxation enhancement of spin labels in membranes by paramagnetic ion salts: dependence on 3*d* and 4*f* ions and on the anions, J. Magn. Reson. 148 (2001) 221–237.
[48] C. Altenbach, D.A. Greenhalgh, H.G. Khorana, W.L. Hubbell, A collision gradient method to determine the immersion depth of nitroxides in lipid bilayers: application to spin-labeled mutants of bacteriorhodopsin, Proc. Natl. Acad. Sci. U. S. A. 91 (1994) 1667–1671.
[49] D. Marsh, Polarity and permeation profiles in lipid membranes, Proc. Natl. Acad. Sci. U. S. A. 98 (2001) 7777–7782.
[50] D.R. Lide, Handbook of Chemistry and Physics, CRC Press, Boca Raton, FL, 1990.
[51] K. Strzalka, T. Sarna, J.S. Hyde, ESR oxymetry: measurement of photosynthetic oxygen evolution by spin-probe technique, Photobiochem. Photobiophys. 12 (1986) 67–71.
[52] W.K. Subczynski, J.S. Hyde, A. Kusumi, Effect of alkyl chain unsaturation and cholesterol intercalation on oxygen transport in membranes—a pulse ESR spin labeling study, Biochemistry 30 (1991) 8578–8590.
[53] A. Ligeza, A. Tikhonov, J. Hyde, W. Subczynski, Oxygen permeability of thylakoid membranes—electron paramagnetic resonance spin labeling study, Biochim. Biophys. Acta 1365 (1998) 453–463.
[54] D. Marsh, Handbook of Lipid Bilayers, CRC Press, Boca Raton, FL, 1990.
[55] X.P. Liu, M.J.S. Miller, M.S. Joshi, D.D. Thomas, J.R. Lancaster, Accelerated reaction of nitric oxide with O_2 within the hydrophobic interior of biological membranes, Proc. Natl. Acad. Sci. U. S. A. 95 (1998) 2175–2179.
[56] C. Altenbach, T. Marti, H.G. Khorana, W.L. Hubbell, Transmembrane protein structure: spin labelling of bacteriorhodopsin mutants, Science 248 (1990) 1088–1092.
[57] W.L. Hubbell, C. Altenbach, Investigation of structure and dynamics in membrane proteins using site-directed spin labeling, Curr. Opin. Struct. Biol. 4 (1994) 566–573.
[58] D. Marsh, T. Páli, L.I. Horváth, Progressive saturation and saturation transfer EPR for measuring exchange processes and proximity relations in membranes, in: L.J. Berliner (Ed.), Spin Labeling. The Next Millenium., vol. 14, Plenum, New York, 1998, pp. 23–82.